

Gas bubble photonics: Manipulating sonoluminescence light with fluorescent and plasmonic nanoparticles

Ivan S. Maksymov 

Optical Sciences Centre, Swinburne University of Technology, Hawthorn, Victoria 3122, Australia

* Correspondence: imaksymov@swin.edu.au ; Tel.: +61-3-3921-4805

Abstract: Oscillations of gas bubbles in liquids irradiated with acoustic pressure waves may result in an intriguing physical phenomenon called sonoluminescence, where a collapsing bubble emits the light in a broad optical spectral range. However, the intensity of the so-generated light is typically weak for practical purposes. Recently, it has been demonstrated that nanoparticles can be used to increase the efficiency of sonoluminescence, thereby enabling one to generate the light that is intense enough for a number of applications in photonics, biomedicine and material science. In this article, we review the latest achievements in the field of nanoparticle-enhanced sonoluminescence and showcase the perspectives of their practical applications.

Keywords: gas bubble; oscillations; cavitation; sonoluminescence; photonics; biophotonics; fluorescence; plasmonics; Purcell effect; metamaterials

1. Introduction

A soap bubble floating in the air, air bubbles rising from a scuba diver in water and bubbles of gas rising in a soft drink are just a few examples of one remarkable physical phenomenon that most of us know since our childhood [1,2]. We can see an air bubble in water because the optical refractive index of air is approximately 1 but that of water is approximately 1.33, which, according to Snell's law [3], allows identifying a bubble due to the effect of optical refraction [4] and internal reflection processes [5].

However, in many natural phenomena and human-made technologies bubbles are rather undetectable with a human eye. Indeed, although the ability of bubbles to affect light has been exploited in atmospheric and marine sciences [6,7] and optical sensing systems [8,9], bubbles have mostly been the subject of extensive studies in the fields of acoustics, fluid dynamics, biomedicine, chemistry and material science, where their size falls mostly within the micron range [10]. For example, artificial microbubbles have been employed in modern biomedical technologies including drug delivery [11–13] and contrast-enhanced medical ultrasound imaging procedures [12,14,15]. Ultrasound contrast agents rely on the ability of spherical bubbles to periodically expand and collapse (oscillate) [Fig. 1(a)] when they are irradiated with ultrasound waves. Commercially available contrast media are specially-prepared lipid-coated microbubbles that can be administered intravenously to the systemic circulation [11–14] and that change the way ultrasound waves are reflected from bodily tissues and fluids. Oscillating bubbles of similar size and composition can be used to deliver drugs to hard-to-reach places inside a living body [Fig. 1(b)], which is, for example, the case of drug delivery through the blood-brain barrier (BBB) that protects the brain against circulating toxins and pathogens causing its infections [16]. We note that the bubble in the middle of the blood vessel in Fig. 1(b) highlights another physical regime of bubble oscillation and collapse suitable for opening BBB and delivering drugs through it, where the bubble collapses non-spherically forming a powerful jet [17–19]. The physics of non-spherically collapsing bubbles is more complex but, in general, similar to that of spherically collapsing bubbles that we discuss in continuation.

Maksymov, I. S. Gas bubble photonics.
Preprints 2022, 1, 0. <https://doi.org/>

Received:
Accepted:
Published:

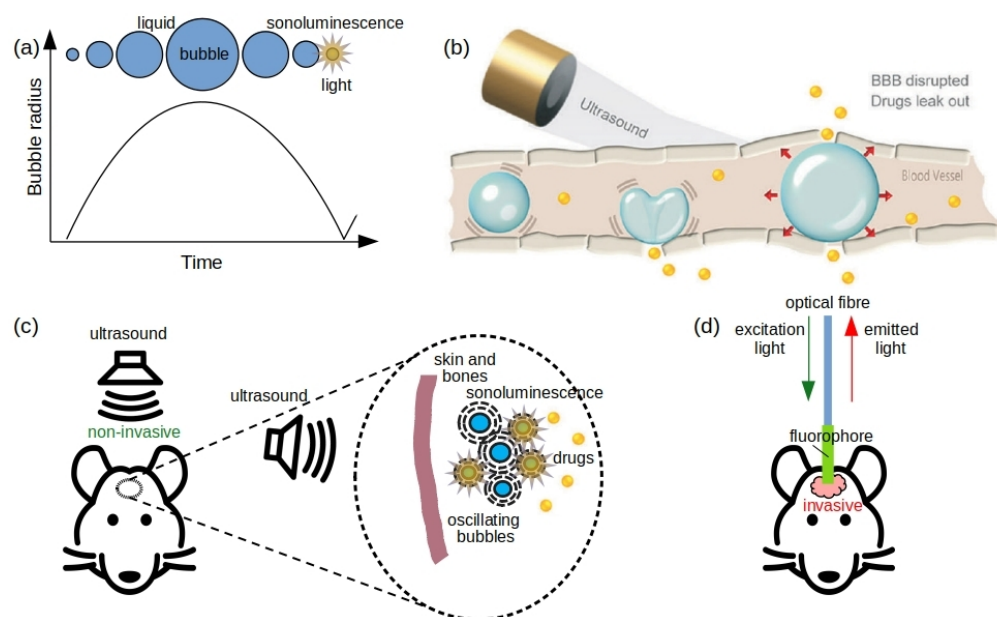


Figure 1. (a) Schematic radius-vs-time diagram for a gas bubble oscillating in the bulk of water. Bubble shapes at different times are shown above the curve during a single oscillation cycle. The pressure inside a bubble is high at the beginning and at the end of the oscillation cycle and is low in the middle. (b) Illustration of the principle of drug delivery through the blood-brain barrier (BBB) using gas bubbles inside a small blood vessel of the brain. Bubble oscillations are driven by an ultrasound wave transducer located outside the head and the drug (small spheres in the picture) pass through the wall of the blood vessel when the bubble either reaches its maximum radius or collapses and forms a water jet. Reproduced from [12] under the terms of a Creative Commons license. (c) Sketch of a potential scheme of drug delivery with gas bubbles and subsequent drug photoactivation with sonoluminescence UV spectral range light. Note a non-invasive nature of this procedure since ultrasound waves needed to trigger the bubble collapse and sonoluminescence can safely pass through the skin, bones and bodily fluids. (d) Illustration of an idealised fluorescence-based fibre-optic probe that can be used for imaging, sensing and drug photoactivation inside a living body. Note that using this technique requires inserting an optical fibre into the body, i.e. this approach requires a surgical intervention.

Apart from their applications in biomedicine, bubbles have also been used for texture tailoring in food industry [20], natural gas recovery in petroleum industry [21], material synthesis in material sciences [22], lab-on-a-chip devices [23], wastewater treatment systems [24], sonochemistry (enhancement and alternation of chemical reactions by means of ultrasound) [25,26], sonoprocessing [25,27] and underwater acoustic communication [28,29]. Moreover, it has been hypothesised that acoustic and fluid-mechanical properties of bubbles in the primordial ocean might contribute to the origin of life on Earth [30] and that the presence of bubbles in the brain and their collapse might be associated with blast-induced neurotraumas [31,32]. The physics of gas bubbles is also relevant to processes taking place during underwater explosions [33].

However, the aforementioned list of properties and practical applications of bubbles is complete. In this article we focus on the well-established capability of an oscillating bubble to emit light in a broad optical spectral range via the process called sonoluminescence [34–38]. As schematically shown in Fig. 1(a), while a bubble in the bulk of liquid periodically expands and collapses under the pressure of an ultrasound wave, at certain experimental conditions the shrinkage of the bubble can result in the emission of pulses of light [34,35]. The

intensity of the emitted light is typically higher in experiments involving individual bubbles [35] compared with the case of multibubble sonoluminescence [38], where the brightness of sonoluminescence is adversely affected by interactions between neighbouring bubbles. In fact, while the light emitted by a single air bubble oscillating in a water-filled glass flask can be seen with the naked eye in a darkened room when using low-power kHz-range ultrasound pressure waves [35], visible multibubble sonoluminescence is possible mostly using high-frequency high-intensity ultrasound waves and bubbles that contain noble gases such as xenon [34].

Moreover, since sonoluminescence light has a significant spectral ultraviolet (UV) component [34,35,39] but bubble oscillations resulting in sonoluminescence can be triggered by ultrasound waves that can pass through the body without noticeable attenuation, it has been argued [40,41] [Fig. 1(c)] that sonoluminescence light can be exploited to noninvasively photoactivate drugs inside a living body in hard-to-reach organs such as the brain. Such ideas are of immediate relevance to the current research efforts in the field of photopharmacology that aims to develop smart drugs that, through the incorporation of molecular photoswitches, enable the remote spatial and temporal control of bioactivity by light [42,43]. This concept is particularly beneficial in the treatment of bacterial infections, where there exists the need of controlling the side effects of antibiotics. However, its practical implementation faces several problems since modern light-responsive drugs mostly rely on UV light, which is a problem because UV radiation is strongly attenuated by bodily fluids and tissues but increasing its intensity results in adverse phototoxic effects on biological cells. These challenges motivate the research on novel drugs that could be activated using red light that falls within the so-called therapeutic window [43], where light has its maximum depth of penetration in tissue [44]. However, using sonoluminescence one might generate UV light directly inside the body, thus resolving the problem of light delivery to the body interior from an external source of UV radiation and also enabling one to use the already discovered UV-sensitive drug compositions. Yet, it has been theoretically shown that sonoluminescence UV light generated inside an internal body organ may have an additional antibacterial effect [39] that can improve the overall performance of UV-activated drugs.

More broadly speaking, using sonoluminescence in the field of biomedicine may be advantageous compared with well-established optical sensing, imaging and drug activation techniques [45], including fluorescence-based methods [46,47], where the use of laser beams and optical fibre probes [Fig. 1(d)] implies that a surgical intervention is needed to access an internal organ such as the brain. On the contrary, a sonoluminescence-based approach may be fully noninvasive since it could rely on advances in the well-established field of conventional medical and transcranial ultrasound imaging methods, where imaging of internal organs and noninvasive functional brain studies are enabled by microbubble-based contrast agents [48].

Fluorescence-based techniques rely on fluorophores—molecules or nanoparticles—that can be applied directly to live specimens to investigate the interior of a cell *in situ* or an internal body organ *in vivo* [45,47]. The light absorption by a fluorophore is followed by re-emission of a photon with a lower energy and a longer wavelength. Hence, fluorescence-based techniques separate the re-emitted lower intensity light from its excitation counterpart creating an image or enabling one to detect chemical composition [49] and temperature [45,50].

However, despite their technological maturity, fluorescence-based approaches have several other notable disadvantages apart from the aforementioned invasive nature of fluorescent probes. Firstly, the operating time of fluorescent molecules, such as those that cover the tip of the probe in Fig. 1(d) [49], is often insufficient for real-time monitoring due to the physico-chemical effect called photobleaching [47]. This problem cannot be simply resolved by increasing the intensity of the excitation light since doing so may cause photodamage to biological cell [51]. While novel fluorescent nanoparticles that require less intense excitation light and that are less prone to photobleaching have been developed [47], their long-term

effect on the cell physiology has not been studied in much detail yet. Therefore, their practical use remains very limited [47]. Yet, the use of fluorescence-based approaches during *in vitro* fertilisation (IVF) poses significant problems—since their effect on the embryo development is unknown, a direct contact of fluorophores with an embryo is ethically unsound and is not permitted in many regulatory jurisdictions [49].

These disadvantages are not expected to exist in sonoluminescence-based approaches. For example, continuing the discussion of the very important and ethically challenging field of IVF, it is well-known that both low-intensity ultrasound waves [52] and microbubble ultrasound contrast agents are safe for obstetric imaging applications [53]. Therefore, it is plausible that bubble-based techniques that produce light would be also suitable for applications in this field. Similarly, sonoluminescence could be achieved using bubbles that serve as ultrasound contrast agent in intravascular imaging procedures [54], where it has been demonstrated that the same bubbles that provide contrast for ultrasound waves used for imaging purposes can be laden with drugs [55,56]. Subsequently, it is conceivable that sonoluminescence light could be used to photoactivate drugs that cover the surface of sonoluminescing microbubbles.

However, the implementations of the idea of sonoluminescence-activated drugs and of relevant proposals have thus far faced a number of fundamental physical and technical limitations—the intensity of the brightest sonoluminescence light attainable in carefully planned and executed experiments is rather low compared with that used in fluorescence-based and similar techniques. Indeed, in a typical single-bubble sonoluminescence experiment involving a sub-millimetre-sized bubble in a water-filled flask that serves as a resonator for kHz-range ultrasound waves, the liquid has to be purified and degassed, the peak pressure amplitude of ultrasound has to reach an optimal value but the bubble has to be created and placed in an exact location inside the flask [34,35]. Given this complexity, for a long time it was assumed that such experimental conditions could not be fulfilled in any scenario of a bubble trapped in a biological fluid, where the chemical composition of the fluid can be highly variable and there would be more many oscillating bubbles that interact one with another [57]. Nevertheless, recently it has been shown that sonoluminescence can be observed under medically relevant conditions using microbubbles commonly employed as contrast agents for ultrasound imaging [40]. At the same time, recent works [39,58,59] also proposed several novel approaches to enhancement of sonoluminescence light intensity to a level that is detectable by standard equipment and is also suitable for photoactivation of drugs [42,43]. In particular, it was shown that the presence of nanoparticles, which does not affect acoustic properties of a bubble, amplifies sonoluminescence by fluorescence-like [58–60] [Fig. 2(a)] and plasmonic [39] effects [Fig. 2(b, c)]. Thus, these results strongly speak in favour of the concept sonoluminescence therapy and photoactivation of drugs [41], especially because plasmonic nanoparticles have played an important role in biomedical technologies [61] and, therefore, their application in sonoluminescence-based technique should help resolve several important problems such as biocompatibility and ethics of use in *in vivo* settings.

2. Discussion

In this section, we review the results of key works relevant to the mainstream discussion in this article. We note that multibubble sonoluminescence was discovered in the 1930s [63,64] and that this phenomenon has been studied in great detail since then [38,65]. Single-bubble sonoluminescence was discovered in the late 1980s [35,66], although according to some sources [38] the very first observation of this effect was reported in 1962 [67]. One remarkable observation made in single-bubble sonoluminescence measurements was the fact that the brightness of light emitted by a bubble was detectable with the naked eye [35]. Yet, the equipment required to observe this effect employed relatively simple electronics. Compared with a much low brightness of light emitted in typical multibubble sonoluminescence experiments that require

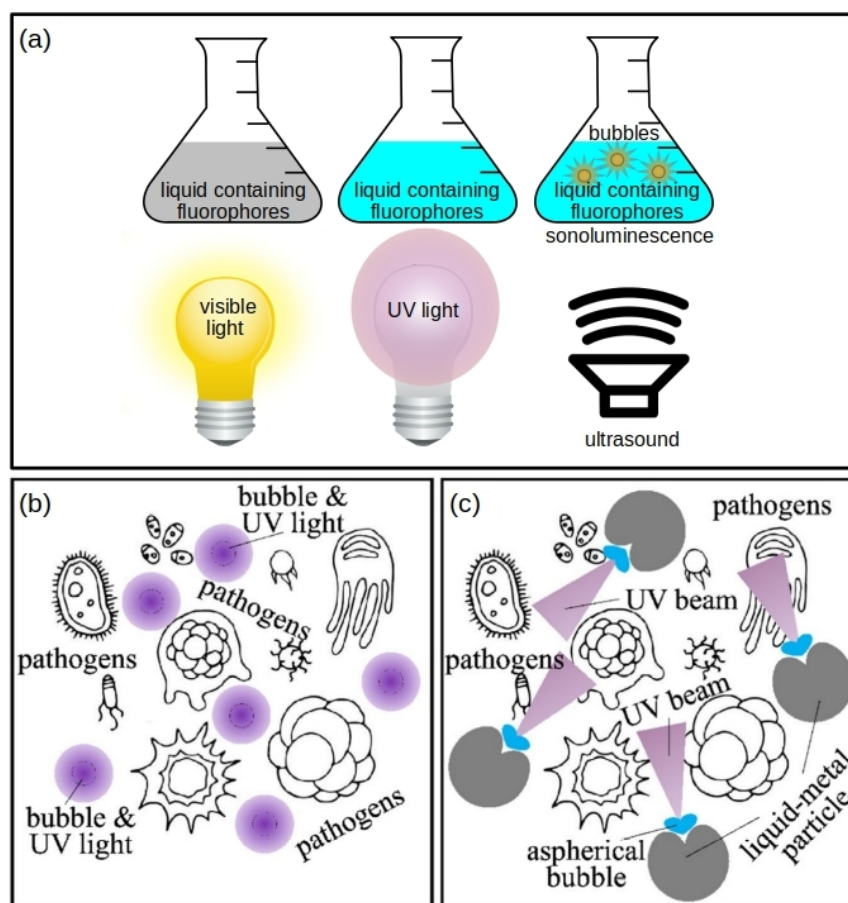


Figure 2. (a) Sketch of a potential proof-of-principle experiment involving a flask filled with water that contains a fluorescent material. When the flask is illuminated with visible light the liquid does not change its colour. However, when the flask is illuminated with UV light the liquid changes its colour due to fluorescence processes. In the rightmost image, the liquid in the flask contains bubbles and it is irradiated with ultrasound, which leads to the emission of sonoluminescence light. Since the so-generated light has a significant UV component, fluorescence processes result in a change in the colour of the liquid. Quinine—a flavour component of tonic water—may be used to realise this experiment since it is known to absorb UV light with the wavelength of around 350 nm and to emit a bright blue light at around 460 nm. As shown in the main text, other suitable chemicals, including luminol, can also be employed. (b, c) The intensity of sonoluminescence light can be enhanced using plasmonic properties of metal nanoparticles that originate from coupling of light to a resonant oscillation of conduction electrons at the metal surface [61,62]. This approach was theoretically demonstrated in [39] in the context of disinfection of water contaminated by pathogens. It was shown that while the intensity of UV light emitted by spherically collapsing gas bubbles is insufficient for UV germicidal irradiation [panel (b)], sonoluminescence associated with aspherical bubble collapse near a metal particle should result in the formation of a UV light beam [panel (c)] that is intense enough for inactivating 99.9% of most common pathogens. Reproduced from [39] under the terms of a Creative Commons license.

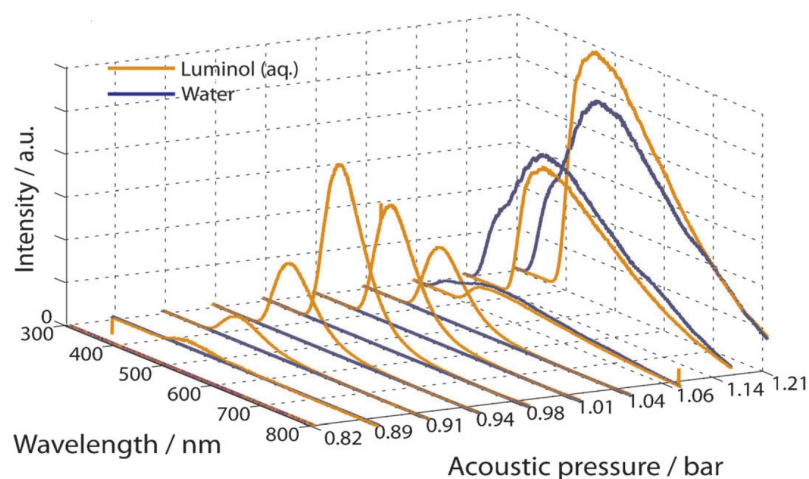


Figure 3. Single-bubble sonoluminescence emission spectra obtained in degassed water compared with the sonochemiluminescence spectra from an aqueous luminol solution. All spectra are plotted as a function of the driving acoustic pressure. Reproduced from [60] with permission of John Wiley and Sons. Copyright 2012.

more complex high-power acoustic power setups, the single-bubble sonoluminescence effect immediately attracted considerable attention of researchers due to its promising potential practical applications. Thus, it is plausible that ideas of using sonoluminescence light for biomedical purposes could be expressed at the same time. Furthermore, in the late 1980s several workers in the field of bubble acoustics and fluid dynamics initiated the studied of cavitation processes using therapeutic ultrasound [68,69] (also note a relevant earlier work, where cavitation and sonochemiluminescence was investigated using high-kHz acoustic pressure waves [70]). This fact also speaks in favour of the assumption that the researchers aimed to use sonoluminescence for medical purposes in the 1980s. On the other hand, according to [41] the first evidence of a biomedical application of sonoluminescence was given in the work [71] that was published in a medical journal, where the authors proposed using sonoluminescence in blood plasma to detect tuberculosis and cancer of the lungs.

However, even though the pioneering experiments on sonoluminescence employed sophisticated experimental equipment, the progress in the field of scientific instrumentation and data processing made in the past decades has enabled new approaches to manipulation of bubbles and detection of light emitted by them. Yet, the last three decades has also seen a dramatic progress in the fields of medicine, chemistry and pharmacology, where, for example, bubbles have been used as ultrasound contrast agents and as a means of targeted drug delivery (see Sec. 1). Alongside the advances in the adjacent areas of sonochemistry, sonoprocessing and sonoporation [25,26,72,73], these factors explain the recent surge in the interest in sonoluminescence from the point of view of biophotonics, imaging and drug discovery [39–41,58].

We start with the discussion of a sonoluminescence regime that can be characterised as an intermediate type of bubble cavitation that bears signatures of both single and multibubble behaviour. In particular, this regime exploits the property of an oscillating bubble to ‘dance’ [57], i.e. to undergo erratic spatial translation movement on a microscopic scale due to Bjerknes force [74,75] (primary Bjerknes force is caused by an external acoustic pressure field but secondary Bjerknes force arises between several bubbles that oscillate in the same acoustic pressure field). While the optical frequency spectrum of the sonoluminescence signal produced by a dancing bubble was found to contain emission lines that are also present in a typical multibubble sonoluminescence spectrum, it was also shown that sonochemical reactions

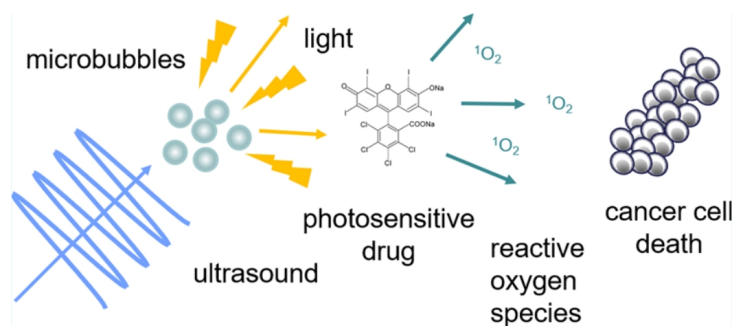


Figure 4. Sketch of the operation of a sonoluminescence-activated photosensitive drug. Note that the use of ultrasound waves enables employing this approach both for diagnostic and therapeutic applications, thereby increasing the range of applications of photosensitive drugs that is currently restricted by a limited penetration of light in the biological tissues and bodily fluids. Reproduced from [40] under the terms of a Creative Commons license.

were possible when luminol—a chemical that fluoresces upon oxidation—was added to the liquid [76]. However, such reactions were not observed in the case of single bubble sonoluminescence.

The emission of light from luminol in a single-bubble experiment was also investigated in [60] at different peak amplitudes of the driving acoustic pressure waves. The results were compared with the data obtained using bubbles in degassed water (Fig. 3). It was shown that while the behaviour of a single bubble in water followed a typically observed light emission pattern, where the onset of strong broadband sonoluminescence occurs at the peak acoustic pressure of about 1.05 bar and then the light intensity increases sharply, in a luminol solution a typical emission band centred at the optical wavelength of 425 nm was observed at significantly lower acoustic pressures from 0.90 to 1.05 bar. It is noteworthy that this form of sonoluminescence is chemical in nature and hence, generally speaking, distinct from conventional sonoluminescence since it occurs in the solution surrounding the collapsing bubble through an oxidative radical process [77]. However, this result is important in the context of the mainstream discussion in this article since it demonstrates that sonoluminescence-like processes can be amplified using luminescent chemicals and that bright light emission can be achieved using ultrasound waves of a lower amplitude compared with sonoluminescence in degassed water. This also means that sonoluminescence could be achieved under medically relevant ultrasound exposure conditions, where the acoustic pressure levels are lower than those used in studies of fundamental sonoluminescence properties.

The ability to achieve multibubble sonoluminescence using therapeutic ultrasound of a relatively low intensity was also demonstrated in [40], where it was also shown that the intensity of so-generated sonoluminescence light could be high enough to activate a photodynamic therapy (PDT) agent (Fig. 4). The latter result is particularly important for the field of photodynamic therapy, where it has been suggested that sonoluminescence and the reactive oxygen species (ROS) associated with bubble collapse could be employed to activate drugs developed in the framework of sonodynamic therapy (SDT) [78,79]. SDT has demonstrated promising results for the treatment of aggressive and resistant tumour cells, and it has several advantages over PDT. For example, while PDT is clinically approved for the treatment of superficial lesions that can be reached with an endoscope [45], a large penetration depth of ultrasound into biological tissues, compared with that of light, enables using SDT in hard-to-reach places in a living body.

However, it is noteworthy that in the experiment in [40] the authors had to use photomultiplier tubes (PMTs) to measure the intensity of sonoluminescence light. PMTs are a class of vacuum tubes that are extremely sensitive detectors of light due to their high gain, low noise, ultra-fast response and large area of collection [80]. While PMTs are more complex and expensive compared with semiconductor-based photodetectors, they remain essential for applications requiring high-sensitivity detection of imperfectly collimated light, which is the case of many multibubble sonoluminescence experiments, especially when the amplitude of ultrasound waves is not high. Although the use of PMTs is not a limiting factor in fundamental research studies, in practice it is desirable to increase the intensity of sonoluminescence light to a level detectable with semiconductor devices.

Since the amplitude of ultrasound waves used for biomedical applications cannot be increased beyond certain limits dictated by particular applications [81], it has been suggested that low-intensity sonoluminescence light generated using ultrasound waves of a relatively low amplitude can be effectively amplified using some of the methods of nanophotonics, where nanoparticles with certain optical properties have been employed both to increase the intensity of light and to manipulate light, for example, by changing its wavelength (colour) [9]. This approach has been validated in the work [58], where functionalised semiconductor ZnO nanoparticles were employed to increase the intensity of sonoluminescence light, reduce the cavitation threshold and promote sonochemical reactions. Combined together, these effects of ZnO nanoparticles enabled decreasing the amplitude of ultrasound waves needed to observe bright sonoluminescence. It is also noteworthy that ZnO nanocrystals have been used in various biomedical fluorescence assays [82], which additionally justifies their application in the experiments in [58] and their suitability for applications in the fields of biology and medicine.

ZnO nanoparticles were synthesised using a microwave-assisted synthesis technique and then they were amine-functionalised to obtain ZnO-NH₂ nanoparticles that exhibited stable colloidal suspensions in both ethanol and distilled water. In the first series of experiments, the sonoluminescence light emission was detected using a PMT under dark conditions. The cavitation threshold was recorded by increasing the amplitude of the ultrasound wave until the appearance of spikes in the PMT-recorded optical spectrum caused by sonoluminescence. The so-recorded cavitation threshold in pure water was about 20% of the maximum power of the ultrasonic transducer used in the measurements and, in agreement with the previous work [83], it was observed that the presence of ZnO-NH₂ nanoparticles in the liquid resulted in a noticeable decrease in the cavitation threshold.

As a next step, sonoluminescence emission in the presence of ZnO-NH₂ nanoparticles was measured using a standard spectrometer capable of detecting light in the spectral range from UV to infrared wavelengths. Since the sensitivity of the spectrometer is lower than that of the PMT device used at the first stage of the experimentation, the acoustic pressure was increased fourfold (however, it constituted about 80% of the maximum power deliverable by the ultrasound transducer used in the measurements).

Figure 5(a) shows the sonoluminescence spectra obtained in pure water as a function of the intensity of the ultrasound wave. One can see a broad frequency peak that is centred around the wavelength of 450 nm and covers the UV and visible spectral ranges. The lowest level of ultrasound intensity that leads to the observation of a clear spectrum—1.2 W/cm²—corresponds to 40% of the maximum ultrasound intensity attainable in the experiment in [58]. However, in the presence of ZnO-NH₂ nanoparticles a clear sonoluminescence spectrum can be observed at a lower ultrasound intensity of 0.9 W/cm² [Fig. 5(b)]. Moreover, one can see that the UV component of the sonoluminescence light (the wavelength from 250 to 350 nm) is absorbed by ZnO-NH₂ nanoparticles. Subsequently, it was verified whether the presence of ZnO-NH₂ could result in a complete absorption of light in the UV range with

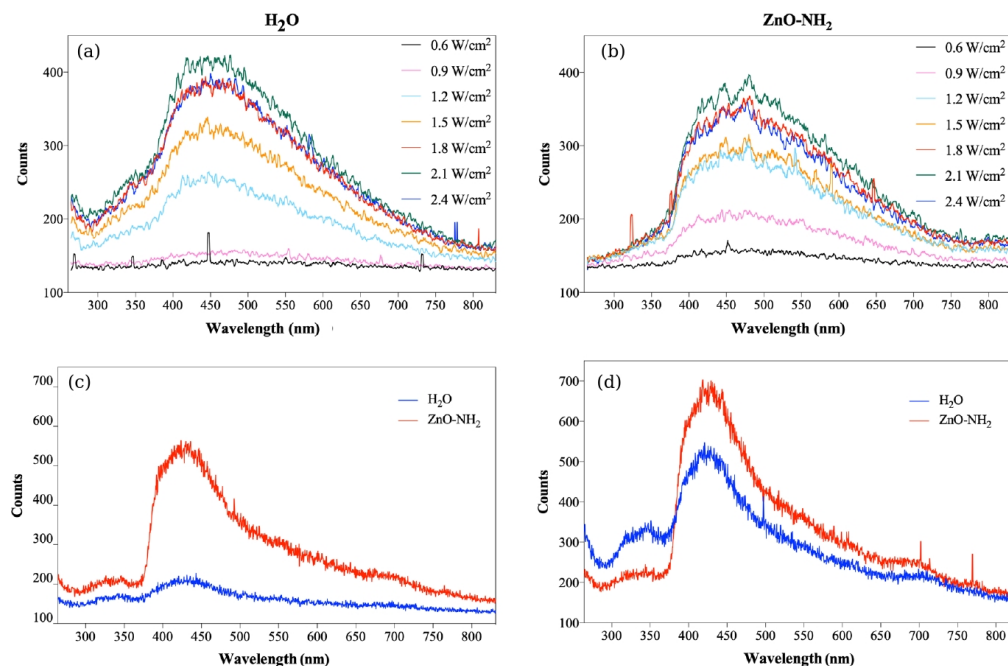


Figure 5. Sonoluminescence light spectra in (a) pure water and (b) in water containing ZnO-NH₂ nanoparticles for different levels of ultrasound intensity. (c, d) The same sonoluminescence light spectra as in panels (a) and (b) but measured in an argon-saturated environment at ultrasound intensities of 0.9 W/cm² and 1.2 W/cm², respectively. Note a clear difference between the spectra in the presence and absence of ZnO-NH₂ nanoparticles. Reproduced from [58] under the terms of a Creative Commons license.

a concomitant re-emission of light in the visible light region. To verify this hypothesis, the measurements were repeated in an argon-saturated atmosphere (it is well-known that the presence of argon results in brighter sonoluminescence [34,35]). The obtained spectra are shown in Fig. 5(c, d) convincingly confirm a strong absorption of UV light by ZnO-NH₂ nanoparticles. However, those results do not confirm any significant re-emission since the spectrum of sonoluminescence light contains high-amplitude frequency components in the entire visible spectral range that may obscure the re-emitted light signal.

Interestingly, it has been shown that multibubble sonoluminescence processes in alcohol can be used to synthesise ZnO and ZnO-coated titanium dioxide nanoparticles [84]. In particular, multibubble sonoluminescence facilitates the supercritical state of liquid layer, thus promoting high-energy chemical reaction in the layer around the bubble. Hence, at optimised multibubble sonoluminescence condition in alcohol solutions containing zinc acetate dihydrate, sodium hydroxide and TiO₂, ZnO nanoparticles with an average diameter of 7 nm were synthesised [84].

Carbon nanodots—nanoscale particles of carbon that have been used as a fluorescent materials that exhibit high biocompatibility and photostability as well as low toxicity and eco-friendliness [47,85,86]—are another type of nanoparticles that can be used to modify the spectrum of sonoluminescence light [59]. In the cited paper, sonoluminescence was achieved in a single-bubble experimental arrangement, where the emission of light is accompanied by the sonochemical reaction $H_2O \rightarrow H^\bullet + OH^\bullet$. The spectrum of light emitted by a single air bubble in water typically extends from from UV to visible wavelengths but its intensity decreases with increasing wavelength, thus explaining observations of light-emitting bubbles as bright blue spots in otherwise dark water. Yet, at relatively low levels of driving acoustic

pressure waves, a characteristic optical spectral line corresponding to OH^\bullet appears in the sonoluminescence spectrum when deionised water is mixed with a noble gas such He, Ar and Xe [34,35]. It is also well-known that certain chemical reactions between OH^\bullet and other chemicals (e.g. luminol as demonstrated in the multibubble experiment in [87]) can help achieve control over sonoluminescence spectra. In the case of carbon nanodots, in one of the experiments reported in [59] it was demonstrated that while the carbon cores of carbon nanodots are changed due to a combined mechanical and thermal effects of sonoluminescence, the chemical groups attached to the surface of carbon nanodots also become modified, which, in turn, changes the optical properties of the nanodots and shifts the broad peak of the sonoluminescence spectrum towards the visible range.

To conclude this section, we review the results of a series of experimental and theoretical works, where it has been suggested that biocompatible micro- and nanoparticles made of non-toxic room-temperature liquid metal alloys can be used to enhance the intensity of the UV component of sonoluminescence light by means of plasmonic effects [30,39,88–91]. Surface plasmons are optical wave that can be resonantly excited at the interface between a metal and a dielectric material [62]. Localised surface plasmon modes are typically observed at the surface of metal nanoparticles, where the plasmon resonance frequency depends on the nanoparticle size, its constituent material and the optical properties of the surrounding environment, but the intensity of light confined to nanoparticle's surface can be higher than that of the incident light due to local optical field enhancement processes [9,61,92].

Nanoparticles suitable for applications in plasmonics are often made of gold and silver since these two metal exhibit the lowest possible optical absorption losses compared with other metals such as nickel and iron [93,94]. However, metals other than gold and silver remain valuable in the field of plasmonics because their use may help extend the functionality of nanoparticles. Indeed, plasmon resonances of typical gold and silver nanoparticles lie in the visible and infrared spectral ranges but their resonance frequencies cannot be readily changed because achieving this would require modifying the shape, size and constituent material of the nanoparticle [61]. Yet, even though there exist techniques for tuning the resonance frequency of a nanoparticle using, for example, magnetic fields [61], the achievable tuning spectral range is insufficient to shift the resonance from the visible to UV spectral range.

To resolve this problem, nanoparticles made of gallium and other metals have been investigated for their UV plasmonic properties (see [91] and references therein). In particular, nanoparticles made of gallium alloys stand out for their intriguing properties that include strong plasmon resonances in the UV spectral range, non-toxicity and biocompatibility as well as the fact that certain gallium alloys can be liquid at room temperature [30,88–90]. Subsequently, compared with solid-metal nanoparticles that have a constant plasmon resonance frequency, the plasmon resonance frequency of liquid gallium alloy nanoparticles can be readily changed using external electric signals [89]. Yet, it has been suggested that liquid metal nanoparticles and larger structures such as macroscopic liquid metal drops could be deformed using acoustic pressure waves [95] and collapsing bubbles [9]. Indeed, let us recall that non-spherically collapsing bubbles (see the bubble in the middle of Fig. 1(b) for illustration) can produce a powerful water jet [18]. The direction of the water jet depends on mechanical properties of the surface near which the bubble collapses. The bubble develops a jet directed towards a rigid surface but away from a liquid-air interface. Yet, the jet splits near an elastic wall [96,97].

In the work [39], it was suggested that the collapse of a microbubble near the surface of a macroscopic liquid-metal drop can result in deformation of the surface and formation of a concave structure that can serve as a focusing mirror for UV light. Moreover, it was hypothesises that the bubble collapse can lead to the emission of sonoluminescence light and that the interaction of the so-generated light with the liquid-metal mirror can result

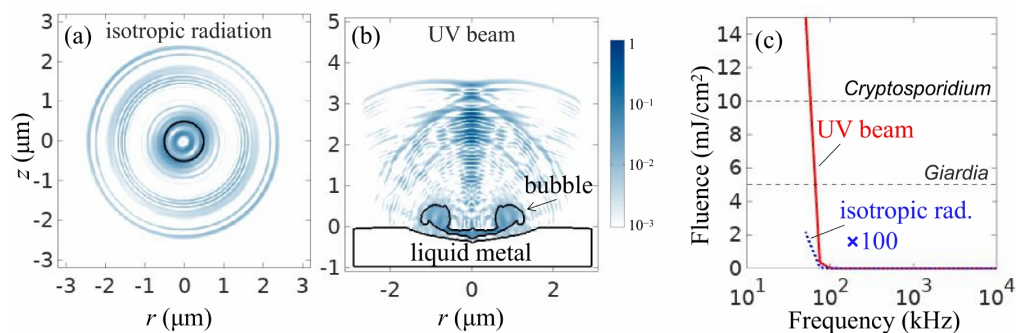


Figure 6. Spatial patterns of light emitted by (a) spherical bubble in a bulk of water and (b) non-spherical bubble near the liquid-metal surface. The black curves outline the contours of the bubble and liquid-metal surface. The equilibrium radius of the bubble is $1 \mu\text{m}$. (c) UV radiation fluence as a function of the ultrasound wave frequency f . The fluence of isotropic radiation is multiplied by 100. The fluence required for the inactivation of *Giardia* and *Cryptosporidium* pathogens is indicated. Reproduced from [39] under the terms of a Creative Commons license.

in the formation of a UV light beam, where the intensity of the UV radiation is increased manifold due to the plasmonic properties of the metal when compared with the intensity of light produced as a result of a spherical bubble collapse. The plausibility of this idea was supported by a rigorous numerical model of microbubble collapse near a liquid metal surface [98,99] and a model of sonoluminescence [35] (compare the result in panels (a) and (b) in Fig. 6).

Although potential applications of this plasmonic enhancement effect in the area of UV photoactivated drugs were not considered in [39], it has been suggested that sonoluminescence-based UV beams could be used to irreversibly inactivate most common pathogens in water. Applying the Fourier transform to spatial patterns of light created by the collapsed spherical [Fig. 6(a)] and non-spherical [Fig. 6(b)] bubbles, it was shown that the time-domain optical wave packets produced by the bubbles carry the spectral radiance for the UV-C wavelengths $\lambda = 200 - 280 \text{ nm}$. It is well-known that UV-C light can be employed to inactivate bacteria, viruses and protozoa in environmentally-friendly, chemical-free and highly effective methods of disinfecting and safeguarding water against pathogens responsible for cholera, polio, typhoid, hepatitis and other bacterial, viral and parasitic diseases [100]. As shown in Figs. 6(a, b), a spherical bubble produces an isotropic radiation while its non-spherical counterpart produces a directed beam perpendicular to the liquid metal surface. Figure 6(c) shows that the UV-C light fluence generated by both spherical and aspherical bubbles dramatically increases at driving ultrasound wave frequencies of less than 100 kHz. However, only the formation of a directed beam near the metal microparticles results in the irreversible inactivation of pathogens.

3. Sonoluminescence in microfluidics-based systems

The results reviewed thus far have been achieved in laboratory conditions that are, in general, different from technologies and equipment employed in modern biomedical sensing and imaging devices based on microfluidic systems and adjacent approaches. Microfluidic technologies enable a quick and efficient processing of small quantities of fluids contained in microscopic channels [101]. The reduced turnaround time and increased productivity with a small device footprint facilitate the application of microfluidic devices in a variety of experimental situations but their high portability makes them a technology of choice for point-of-care devices [22,23].

The physical and chemical properties of oscillating and collapsing gas bubbles discussed in this article have also been essential for the development of microfluidic technologies [18,22,102–104]. Therefore, it is plausible that sonoluminescence can be achieved in microfluidics-based system. Indeed, in the work [87] micromachined pits on a solid substrate were employed to nucleate and stabilise microbubbles in a liquid irradiated with an ultrasound pressure wave, and ultrasound-driven collapse of such bubbles resulted in the emission of light. In turn, the generated light interacted with luminol that was present in the liquid, thus producing a sonochemiluminescence effect. The intensities of sonoluminescence and sonochemiluminescence optical signals were recorded at several operating regimes related to the peak acoustic pressure amplitude at the ultrasonic frequency of 200 kHz for a pure water environment and for aqueous luminol and propanol solutions. Several arrangements of pits on the substrate were investigated. At high acoustic pressures and in the presence of more than one pit on the substrate, the microbubbles combined into a chain or formed a triangular structure known as a streamer [18]. In all experiments the intensity of sonochemiluminescence light was amplified as the number of pits was increased. This result was reproducible at both low and high acoustic pressure levels.

In another relevant work [26], the conditions suitable for a realisation of sonoluminescence and sonochemistry were created using bubbles confined within a narrow channel of a microfluidic device [Fig. 7(a)], where the bubbles assume a planar pancake-like shape. As a result of collapse of such bubbles the authors observed the formation of *OH* radicals and the emission of sonoluminescence light [Fig. 7(b)]. The observation of chemical reactions was closely linked to the gas-liquid interfaces [Fig. 7(c)] and it was suggested that spatial control over them could be used to control sonochemical reactions. Furthermore, the decay time of the light emitted from the sonochemical reaction was several orders faster than that in the bulk of liquid and the emission of light vanished immediately as the ultrasound was switched off (also see a relevant discussion of the Purcell effect below).

It has also been shown theoretically that microscopic water-core optical fibre can be used as microfluidic channels, where bubbles may oscillate, collapse and emit light under the pressure of an ultrasound pressure wave [105]. The fibre analysed in [105] consisted of a Teflon tube filled with water. The optical refractive index of Teflon is slightly lower than that of water, which creates the conditions suitable for efficient concentration of light inside the water core. Although optical losses in the water-core fibre are higher than those in modern solid-state fibres, the liquid-based system has certain advantages relevant to the main discussion in this article. In particular, it was demonstrated that the water-core fibre can efficiently guide light when the Teflon tube is immersed into another liquid. Yet, numerical simulations conducted in [105] revealed that ultrasound waves can pass through the structure of the water-immersed fibre with negligibly small acoustic scattering and attenuation. Given these unique properties, it is plausible that sonoluminescence light produced inside the core of the fibre could be efficiently collected and detected using a standard photodetector connected to the output end of the fibre.

4. Conclusions and open questions

In this article, we have reviewed the recent results in the emergent field of fluorescence and plasmonic nanoparticle-enhanced sonoluminescence with a focus on potential applications of light emitted by collapsing bubbles in the fields of photonics and biophotonics and adjacent areas. Given the ability of ultrasound waves that cause the bubble collapse to readily pass through the skin and bodily fluids and tissues, and due to the presence of natural and artificial gas bubbles inside a living body, it has been argued that sonoluminescence light could be used to activate certain drugs inside the body, also providing a means for inactivation of pathogens with UV radiation and for imaging of individual cells without

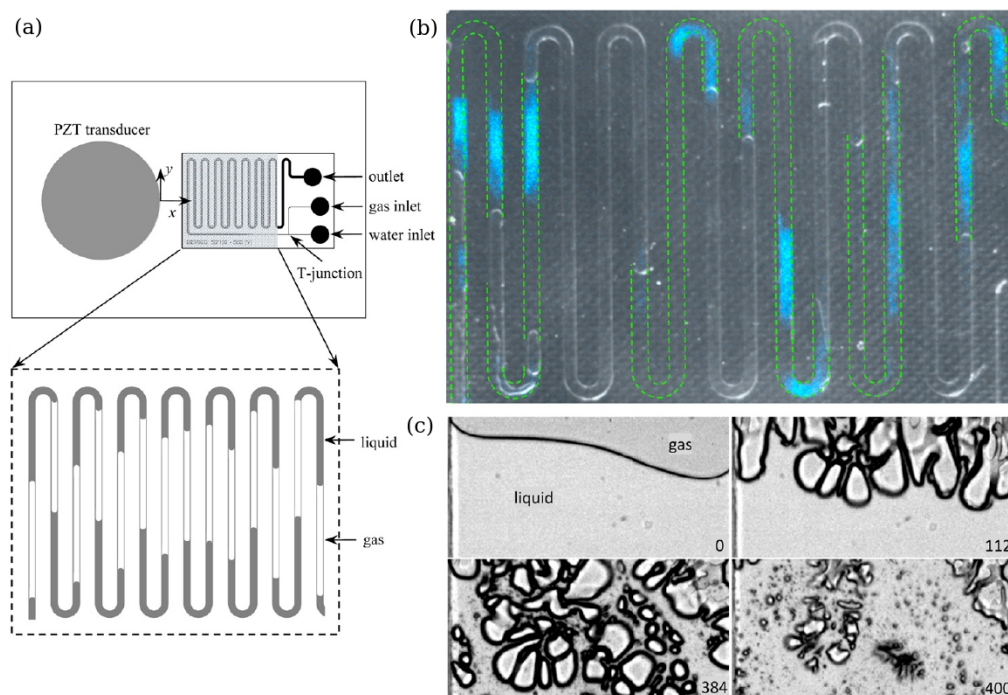


Figure 7. (a) Sketch of the microfluidic device designed in [26] to observe sonochemistry and sonoluminescence effects. The piezoelectric transducer (PZT) used for the creation of the driving ultrasound wave is glued to a glass substrate to which a meandering microfluidic channel is bonded. The inlets consist of two ports for gas and water, respectively. The inset shows a typical distribution of gas and liquids along the microchannel. (b) Picture of the microfluidic channel geometry superimposed on a photograph showing a sonochemiluminescence activity due to the oxidation of luminol. The green dashed lines indicate the positions of liquid slugs inside the channels just before the ultrasound was switched on. (c) Sequence of images taken with a high-speed camera showing the bubble distribution near a gas-liquid interface. The number in each frame is the time in microseconds after switching on the ultrasound signal. One can see that the initial gas-liquid interface leads to surface instabilities, expansions of large bubbles and eventually to bubble collapses. The interface was exposed to a harmonic ultrasound driving wave with the frequency of 103.6 kHz. The width of each frame is 500 μm , which is also the width of the microfluidic channel. Reproduced from [26] under the exclusive PNAS License to Publish. Copyright 2011 National Academy of Sciences.

application of chemicals that can pose ethical issues. While rigorous *in vivo* tests of these potential applications of sonoluminescence have not been conducted yet, the results obtained in a number of recent experimental works, where commercial medical ultrasound imaging microbubble contrast agents and medical-grade ultrasound wave intensities were employed, strongly speak in favour of plausibility of the concept of sonoluminescence-based photonics and biophotonics.

However, extra research studies are required for sonoluminescence-based processes to attract the interest of a large number of scientists working on photonics and biophotonics. Here, we outline the current challenges and open questions the resolution of which, in our opinion, will shape the future research efforts in the area of sonoluminescence and gas bubble photonics.

Firstly, the experiments involving the interaction of sonoluminescence light with nanoparticles have thus far been conducted in purified liquids and liquids that contain chemicals that facilitate observations of bright sonoluminescence. However, in biologically-relevant situations the composition of fluids may be unfavourable for the production of sonoluminescence from the point of view of both fluid dynamics and optics. Therefore, additional studies of sonoluminescence have to be conducted in different types of biofluids or fluids that have similar properties, and the research questions such as the impact of the biofluid viscosity and of light absorption and scattering have to be rigorously addressed. Indeed, while in single-bubble sonoluminescence experiments microbubbles can be trapped in water using standing acoustic pressure waves, achieving a stable bubble position in liquids with higher viscosity has proven to be challenging since in such liquids bubbles undergo a quasiperiodic circular translational motion on the time scale of seconds [106].

Secondly, it is known that the intensity of light emitted by a single sonoluminescing bubble can be increased using several driving ultrasound waves of different frequencies. The optimal values of pressure amplitude and relative phase of the ultrasound waves were reported in [107], where a two harmonic frequency bubble forcing regime—26.5 kHz and 53 kHz—has been shown to result in increased temperatures inside a sonoluminescing bubble that maintained its spherical stability despite the action of two acoustic pressure waves. Subsequently, a combination of this sonoluminescence regime with nanoparticles should allow achieving higher sonoluminescence light intensities. It is also plausible that the use of more than two excitation frequencies or even a quasi-continuum of frequencies would result in strong sonoluminescence provided that the bubble maintains its spherical shape during the oscillation. One potential test of this idea could employ acoustic frequency combs—signals with spectra consisting of equidistant frequency peaks [29]. Despite a multifrequency content of an acoustic frequency comb signal, a bubble driven by it can still maintain its spherical shape [108] that is favourable for producing sonoluminescence [35].

Thirdly, in the field of nanophotonics it is well-established that luminescent quantum emitters have relatively long emission lifetimes of several tens of nanoseconds and non-directional emission patterns. These intrinsic optical properties are not suitable for applications in many nanophotonic devices such as single-photon sources [109], where fast radiative rates are required for operation at high frequencies but directionality is needed to achieve a high efficiency of light collection [110,111]. One of the approaches to the resolution of this problems exploits the Purcell effect—a modification of the spontaneous emission rate of an emitter of light in the presence of a resonant cavity [110–112]. The Purcell effect has also been observed in systems consisting of plasmonic nanoparticles—nanoantennas [61,110–112]—that can modify the photonic environment of fluorescent sources of light by enhancing the spontaneous emission rate.

Given that the physics of sonoluminescence can also be explained in terms of quantum radiation [113,114], it is conceivable that the properties of sonoluminescence-based light sources

could also be controlled using the Purcell effect originating from the plasmonic properties of metal nanoparticles. Moreover, such tests could be conducted in opto-microfluidic channels used in biomedical and pharmaceutical research, where, for example, sonoluminescence of bubbles nucleated in pits formed on a silicon substrate has been reported in [87]. Due to the decent optical properties of silicon, the pits formed in this material possess the properties of optical micro-cavities, where a strong Purcell effect has been observed [110–112]. An enhancement of the sonoluminescence light intensity could also be investigated in an acousto-optical device [115], where a microscopically patterned metallic film simultaneously plays the roles of a bubble-generating substrate and of an optical resonator [109]. Furthermore, the Purcell effect could be used to inhibit the emission of a source of light [110]. Subsequently, from the point of view of the fundamental physics, one might be interested in studying potential effects of light emission inhibition under otherwise favourable conditions for the production of sonoluminescence. Yet, since the existence of acoustic and elastic counterparts of the optical Purcell effect has been demonstrated [116,117], and the possibility of combining the optical and acoustic Purcell effects has been pointed out [118], one might control sonochemiluminescence light intensity using both optical and acoustic techniques.

It is also worth noting that sonoluminescence processes may be of interest to the burgeoning field of metamaterials [119,120]. In general, a metamaterial is any artificial material engineered to have a property that is not found in naturally occurring media. For instance, an electromagnetic metamaterial affects electromagnetic waves that interact with its structural features. Since a typical size of the features of a metamaterial is smaller than the wavelength of the incident wave, photonic metamaterials that operate at optical frequencies are usually structured at the nanometre scale [119]. Similarly, the features of acoustic metamaterials designed to control, direct and manipulate acoustic waves in fluids and solids are typically smaller than the wavelength of the incident acoustic wave [121].

Among different kinds of metamaterials, hyperbolic metamaterials have attracted a special attention since their hyperbolic dispersion relationship gives rise to useful effects including enhancement of spontaneous emission, negative refraction and ability to overcome the optical diffraction limit [120]. The concept of hyperbolic metamaterials has been extended to waves other than electromagnetic waves and light, where, in particular, it has been suggested that acoustic waves existing in hyperbolic metamaterials can be regarded as analogues of gravitational waves [122]. In this context and in light of the theoretical works [113,114] demonstrating a quantum nature of sonoluminescence, it has been suggested that the efficiency of sonoluminescence could be greatly enhanced using hyperbolic metamaterials and that studies of sonoluminescence processes in hyperbolic metamaterials could help search for quantum gravity effects [122]. One suitable candidate for such experimental tests is a ferrofluid-based self-assembled hyperbolic metamaterial, where a chain of cobalt nanoparticles, which leads to formation of the hyperbolic metamaterial structure, and microbubbles are formed inside the ferrofluid after application of external magnetic field [123].

Funding: This work has been supported by the Australian Research Council through the Future Fellowship (FT180100343) program.

Acknowledgments: ISM thanks Professor Sergey Suslov, Dr. Andrey Pototsky and Mr. Bui Quoc Huy Nguyen for their support and invaluable discussions.

Conflicts of Interest: The author declares no conflict of interest.

Abbreviations

The following abbreviations are used in this manuscript:

blood-brain barrier	BBB
<i>in vitro</i> fertilisation	IVF
photomultiplier tube	PMT
photodynamic therapy	PTD
piezoelectric transducer	PZT
reactive oxygen species	ROS
sonodynamic therapy	SDT
ultraviolet	UV

References

- Brennen, C.E. *Cavitation and Bubble Dynamics*; Oxford University Press, New York, 1995.
- Lauterborn, W.; Kurz, T. Physics of bubble oscillations. *Rep. Prog. Phys.* **2010**, *73*, 106501.
- Born, M.; Wolf, E. *Principles of Optics*; Cambridge University Press, Cambridge, 1997.
- Raciti, D.; Brocca, P.; Raudino, A.; Corti, M. Interferometric detection of hydrodynamic bubble-bubble interactions. *J. Fluid Mech.* **2022**, *942*, R1.
- Miller, S.; Ding, Y.; Jiang, L.; Tu, X.; Pau, S. Observation of elliptically polarized light from total internal reflection in bubbles. *Sci. Reps.* **2020**, *10*, 8725.
- Shifrin, K.S. *Scattering of Light in a Turbid Medium*; National Aeronautics and Space Administration, 1959.
- Hansen, G.M. Mie scattering as a technique for the sizing of air bubbles. *Appl. Opt.* **1985**, *24*, 3214–3220.
- Xu, H.; Wang, G.; Ma, J.; Jin, L.; Oh, K.; Guan, B. Bubble-on-fiber (BoF): a built-in tunable broadband acousto-optic sensor for liquid-immersible in situ measurements. *Opt. Express* **2018**, *26*, 11976–11983.
- Maksymov, I.S.; Greentree, A.D. Coupling light and sound: giant nonlinearities from oscillating bubbles and droplets. *Nanophotonics* **2019**, *8*, 367–390.
- Tsuge, H. *Micro- and Nanobubbles: Fundamental and Applications*; Pan Stanford, Singapore, 2014.
- Burgess, A.; Shah, K.; Hough, O.; Hynynen, K. Focused ultrasound-mediated drug delivery through the blood-brain barrier. *Expert. Rev. Neurother.* **2015**, *15*, 477–491.
- Kang, S.T.; Yeh, C.K. Ultrasound microbubble contrast agents for diagnostic and therapeutic applications: Current status and future Design. *Chang Gung Med. J.* **2012**, *35*, 125–139.
- Deng, W.; Chen, W.; Clement, S.; Guller, A.; Zhao, Z.; Engel, A.; Goldys, E.M. Controlled gene and drug release from a liposomal delivery platform triggered by X-ray radiation. *Nat. Commun.* **2018**, *9*, 2713.
- Lindner, J.R. Microbubbles in medical imaging: current applications and future directions. *Nat. Rev. Drug Discov.* **2004**, *3*, 527–532.
- Postema, M.; Gilja, O.H. Contrast-enhanced and targeted ultrasound. *World J. Gastroenterol* **2011**, *17*, 28–41.
- Daneman, R.; Prat, A. The blood-brain barrier. *Cold Spring Harb. Perspect. Biol.* **2015**, *7*, a020412.
- Marston, P.L.; Trinh, E.H.; Depew, J.; Asaki, J. Response of bubbles to ultrasonic radiation pressure: Dynamics in low gravity and shape oscillations. In *Bubble Dynamics and Interface Phenomena*; Blake, J.R.; Boulton-Stone, J.M.; Thomas, N.H., Eds.; Kluwer Academic: Dordrecht, 1994; pp. 343–353.
- Ohl, S.W.; Klaseboer, E.; Khoo, B.C. Bubbles with shock waves and ultrasound: a review. *Interface Focus* **2015**, *5*, 20150019.
- Manasseh, R., Acoustic Bubbles, Acoustic Streaming, and Cavitation Microstreaming. In *Handbook of Ultrasonics and Sonochemistry*; Springer Singapore: Singapore, 2016; pp. 33–68. doi:10.1007/978-981-287-278-4_5.
- Dutta, A.; Chengara, A.; Nikolov, A.D.; Wasan, D.T.; Chen, K.; Campbell, B. Destabilization of aerated food products: effects of Ostwald ripening and gas diffusion. *J. Food Eng.* **2004**, *62*, 177–184.
- May, E.F.; Lim, V.W.; Metaxas, P.J.; Du, J.; Stanwix, P.L.; Rowland, D.; Johns, M.L.; Haandrikman, G.; Crosby, D.; Aman, Z.M. Gas Hydrate Formation Probability Distributions: The Effect of Shear and Comparisons with Nucleation Theory. *Langmuir* **2018**, *34*, 3186–3196.
- Khan, S.A.; Duraiswamy, S. Controlling bubbles using bubbles-microfluidic synthesis of ultra-small gold nanocrystals with gas-evolving reducing agents. *Lab Chip* **2012**, *12*, 1807–1812.
- Hashmi, A.; Yu, G.; Reilly-Collette, M.; Heiman, G.; Xu, J. Oscillating bubbles: a versatile tool for lab on a chip applications. *Lab Chip* **2012**, *12*, 4216.
- Gogate, P. Treatment of wastewater streams containing phenolic compounds using hybrid techniques based on cavitation: A review of the current status and the way forward. *Ultrason. Sonochem.* **2008**, *15*, 1–15.
- Mason, T.J. Sonochemistry and sonoprocessing: the link, the trends and (probably) the future. *Ultrason. Sonochem.* **2003**, *10*, 175–179.
- Tandiono.; Ohl, S.W.; Ow, D.S.W.; Klaseboer, E.; Wong, V.V.; Dumke, R.; Ohl, C.D. Sonochemistry and sonoluminescence in microfluidics. *PNAS* **2011**, *108*, 5996–5998.
- Rubio, F.; Blandford, E.D.; Bond, L.J. Survey of advanced nuclear technologies for potential applications of sonoprocessing. *Ultrasonics* **2016**, *71*, 211–222.

28. Preisig, J. The impact of bubbles on underwater acoustic communications in shallow water environments. *J. Acoust. Soc. Am.* **2003**, *114*, 2370.
29. Maksymov, I.S.; Nguyen, B.Q.H.; Pototsky, A.; Suslov, S.A. Acoustic, phononic, Brillouin light scattering and Faraday wave-based frequency combs: physical foundations and applications. *Sensors* **2022**, *22*, 3921.
30. Kalson, N.H.; Furman, D.; Zeiri, Y. Cavitation-induced synthesis of biogenic molecules on primordial Earth. *ACS Cent. Sci.* **2017**, *3*, 1041–1049.
31. Cernak, I. Understanding blast-induced neurotrauma: how far have we come? *Concussion* **2017**, *2*, CNC42.
32. Barney, C.W.; Dougan, C.E.; McLeod, K.R.; Kazemi-Moridani, A.; Zheng, Y.; Ye, Z.; Tiwari, S.; Sacligil, I.; Riggleman, R.A.; Cai, S.; Lee, J.H.; Peyton, S.R.; Tew, G.N.; Crosby, A.J. Cavitation in soft matter. *PNAS* **2020**, *117*, 9157–9165.
33. Cole, R.H. *Underwater Explosions*; Princeton University Press, New York, 1948.
34. Putterman, S.J.; Weninger, K.R. Sonoluminescence: How bubbles turn sound into light. *Annu. Rev. Fluid Mech.* **2000**, *32*, 445–476.
35. Brenner, M.P.; Hilgenfeldt, S.; Lohse, D. Single-bubble sonoluminescence. *Rev. Mod. Phys.* **2002**, *74*, 425–484.
36. Farhat, M.; Chakravarty, A.; Field, J.E. Luminescence from hydrodynamic cavitation. *Proc. R. Soc. A.* **2011**, *467*, 591–606.
37. Borisenok, V.A. Sonoluminescence: Experiments and models (review). *Acoust. Phys.* **2015**, *61*, 308–332.
38. Yasui, K. Multibubble sonoluminescence from a theoretical perspective. *Molecules* **2021**, *26*, 4624.
39. Boyd, B.; Suslov, S.A.; Becker, S.; Greentree, A.D.; Maksymov, I.S. Beamed UV sonoluminescence by aspherical air bubble collapse near liquid-metal microparticles. *Sci. Rep.* **2020**, *10*, 1501.
40. Beguin, E.; Shrivastava, S.; Dezhkunov, N.V.; McHale, A.P.; Callan, J.F.; Stride, E. Direct evidence of multibubble sonoluminescence using therapeutic ultrasound and microbubbles. *ACS Appl. Mater. Interfaces* **2019**, *11*, 19913–19919.
41. Canaparo, R.; Foglietta, F.; Giuntini, F.; Francovich, A.; Serpe, L. The bright side of sound: perspectives on the biomedical application of sonoluminescence. *Photochem. Photobiol. Sci.* **2020**, *10*, 1114–1121.
42. Velema, W.A.; Szymanski, W.; Feringa, B.L. Photopharmacology: beyond proof of principle. *J. Am. Chem. Soc.* **2014**, *136*, 2178–2191.
43. Wegener, M.; Hansen, M.J.; Driessen, A.J.M.; Szymanski, W.; Feringa, B.L. Photocontrol of antibacterial activity: shifting from UV to red light activation. *J. Am. Chem. Soc.* **2017**, *139*, 17979–17986.
44. Smith, A.M.; Mancini, M.C.; Nie, S. Second window for *in vivo* imaging. *Nat. Nanotech.* **2009**, *4*, 710–711.
45. Li, J.; Eberndorff-Heidepriem, H.; Gibson, B.C.; Greentree, A.D.; Hutchinson, M.R.; Jia, P.; Kostecky, R.; Liu, G.; Orth, A.; Ploschner, M.; Schartner, E.P.; Warren-Smith, S.C.; Zhang, K.; Tsiminis, G.; Goldys, E.M. Perspective: Biomedical sensing and imaging with optical fibers—Innovation through convergence of science disciplines. *APL Photon.* **2018**, *3*, 100902.
46. Tong, R.; Hemmati, H.D.; Langer, R.; Kohane, D.S. Photoswitchable nanoparticles for triggered tissue penetration and drug delivery. *J. Am. Chem. Soc.* **2012**, *134*, 8848–8855.
47. Reineck, P.; Gibson, B.C. Near-infrared fluorescent nanomaterials for bioimaging and sensing. *Adv. Opt. Mater.* **2017**, *5*, 1600446.
48. Errico, C.; Osmanski, B.F.; Pezet, S.; Couture, O.; Lenkei, Z.; Tanter, M. Transcranial functional ultrasound imaging of the brain using microbubble-enhanced ultrasensitive Doppler. *NeuroImage* **2015**, *124*, 752–761.
49. Purdey, M.S.; Thompson, J.G.; Monro, T.M.; Abell, A.D.; Schartner, E.P. A dual sensor for pH and hydrogen peroxide using polymer-coated optical fibre tips. *Sensors* **2015**, *15*, 31904–31913.
50. Musolino, S.; Schartner, E.P.; Tsiminis, G.; Salem, A.; Monro, T.M.; Hutchinson, M.R. Portable optical fiber probe for *in vivo* brain temperature measurements. *Biomed. Opt. Express* **2016**, *7*, 3069–3078.
51. Zablocki, M.; McCormack, K.; van den Hurk, M.; Milky, B.; Shoubridge, A.P.; Adams, R.; Tran, J.; Mahadevan-Jansen, A.; Reineck, P.; Thomas, J.; Hutchinson, M.R.; Mak, C.K.H.; Añonuevo, A.; Chew, L.H.; Hirst, A.J.; Lee, V.M.; Knock, E.; Bardy, C. BrainPhys neuronal medium optimized for imaging and optogenetics *in vitro*. *Nat. Commun.* **2020**, *11*, 5550.
52. Whitworth, M.; Bricker, L.; Mullan, C. Ultrasound for fetal assessment in early pregnancy. *Cochrane Database Syst. Rev.* **2015**, *2015* (7), CD007058.
53. Yusefi, H.; Helfield, B. Ultrasound contrast imaging: fundamentals and emerging technology. *Front. Phys.* **2022**, *10*, 791145.
54. Wang, B.; Su, J.L.; Karpouk, A.B.; Sokolov, K.V.; Smalling, R.W.; Emelianov, S.Y. Intravascular photoacoustic imaging. *IEEE J. Sel. Topics Quantum Electron.* **2010**, *16*, 588–599.
55. Wilson, K.; Homan, K.; Emelianov, S. Biomedical photoacoustics beyond thermal expansion using triggered nanodroplet vaporization for contrast-enhanced imaging. *Nat. Commun.* **2011**, *3*, 618.
56. Dove, J.D.; Murray, T.W.; Borden, M.A. Enhanced photoacoustic response with plasmonic nanoparticle-templated microbubbles. *Soft Matter* **2013**, *9*, 7743–7750.
57. Doinikov, A.A. *Bubble and Particle Dynamics in Acoustic Fields: Modern Trends and Applications*; Research Signpost, Kerala, India, 2005.
58. Vighetto, V.; Troia, A.; Laurenti, M.; Carofiglio, M.; Marcucci, N.; Canavese, G.; Cauda, V. Insight into sonoluminescence augmented by ZnO-functionalized nanoparticles. *ACS Omega* **2020**, *7*, 6591–6600.
59. Song, D.; Xu, W.; Luo, M.; You, K.; Tang, J.; Wen, H.; Cheng, X.; Luo, X.; Wang, Z. Turning single bubble sonoluminescence from blue in pure water to green by adding trace amount of carbon nanodots. *Ultrason. Sonochem.* **2021**, *78*, 105727.

60. Brotchie, A.; Schneider, J.; Pflieger, R.; Shchukin, D.; Möhwald, H. Sonochemiluminescence from a single cavitation bubble in water. *Chem. Eur. J.* **2012**, *18*, 11201–11204.
61. Maksymov, I.S. Magneto-plasmonic nanoantennas: Basics and applications. *Rev. Phys.* **2016**, *1*, 36–51.
62. Raether, H. *Surface Plasmons on Smooth and Rough Surfaces and on Gratings*; Springer-Verlag, Berlin, 1987.
63. Marinesco, N.; Trillat, J.J. Action des ultrasons sur les plaques photographiques. *Proc. R. Acad. Sci. Amst.* **1933**, *196*, 858–860.
64. Frenzel, H.; Schultes, H. Lumineszenz im ultraschall-beschickten Wasser. *Z. Phys. Chem. Abt.* **1934**, *27B*, 421–424.
65. Suslick, K.S.; Flannigan, D.J. Inside a collapsing bubble: sonoluminescence and the conditions during cavitation. *Annu. Rev. Phys. Chem.* **2008**, *59*, 659–683.
66. Gaitan, D.F.; Crum, L.A.; Church, C.C.; Roy, R.A. Sonoluminescence and bubble dynamics for a single, stable, cavitation bubble. *J. Acoust. Soc. Am.* **1992**, *91*, 3166–3183.
67. Yosioka, K.; Omura, A. The light emission from a single bubble driven by ultrasound and the spectra of acoustic oscillation. *Proc. Annu. Meet. Acoust. Soc. Jpn.* **1962**, pp. 125–126.
68. Pickworth, M.J.W.; Dendy, P.P.; Leighton, T.G.; Walton, A.J. Studies of the cavitation effects of clinical ultrasound by conoluminescence: 2. Thresholds for sonoluminescence from a therapeutic ultrasound beam and the effect of temperature and duty cycle. *Phys. Med. Biol.* **1988**, *33*, 1249–1260.
69. Umemura, S.; Yumita, N.; Nishigaki, R.; Umemura, K. Mechanism of cell damage by ultrasound in combination with hematoporphyrin. *Jpn. J. Cancer Res.* **1990**, *81*, 962–966.
70. Srinivasan, D.; Holroyd, L.V. Optical spectrum of the sonoluminescence emitted by cavitated water. *J. Appl. Phys.* **1961**, *32*, 446–449.
71. Zhadnov, V.Z.; Mishanov, R.F.; Chernov, V.V. Sonoluminescence of blood plasma in the differential diagnosis of tuberculosis, cancer and sarcoidosis of the lungs. *Probl. Tuberk.* **1994**, pp. 42–43.
72. Helfield, B.; Chen, X.; Watkins, S.C.; Villanueva, F.S. Biophysical insight into mechanisms of sonoporation. *PNAS* **2016**, *113*, 9983–9988.
73. Yang, Y.; Li, Q.; Guo, X.; Tu, J.; Zhang, D. Mechanisms underlying sonoporation: Interaction between microbubbles and cells. *Ultrason. Sonochem.* **2020**, *67*, 105096.
74. Bjerknes, V. *Fields of Force*; The Columbia University Press, New York, 1906.
75. Crum, L.A. Bjerknes forces on bubbles in a stationary sound field. *J. Acoust. Soc. Am.* **1975**, *57*, 1363–1370.
76. Hatanaka, S.; Mitome, H.; Yasui, K.; Hayashi, S. Single-bubble sonochemiluminescence in aqueous luminol solutions. *J. Am. Chem. Soc.* **2002**, *124*, 10250–10251.
77. McMurray, H.N.; Wilson, B.P. Mechanistic and spatial study of ultrasonically induced luminol chemiluminescence. *J. Phys. Chem. A* **1999**, *103*, 3955–3962.
78. Ninomiya, K.; Noda, K.; Ogino, C.; Kuroda, S.I.; Shimizu, N. Enhanced OH radical generation by dual-frequency ultrasound with TiO₂ nanoparticles: its application to targeted sonodynamic therapy. *Ultrason. Sonochem.* **2014**, *21*, 289–294.
79. Osaki, T.; Yokoe, I.; Uto, Y.; Ishizuka, M.; Tanaka, T.; Yamanaka, N.; Kurahashi, T.; Azuma, K.; Murahata, Y.; Tsuka, T.; Ito, N.; Imagawa, T.; Okamoto, Y. Bleomycin enhances the efficacy of sonodynamic therapy using aluminum phthalocyanine disulfonate. *Ultrason. Sonochem.* **2016**, *28*, 161–168.
80. Wright, A.G. *The Photomultiplier Handbook*; Oxford University Press, Oxford, 2017.
81. Miller, D.; Smith, N.; Bailey, M.; Czarnota, G.; Hynynen, K.; Makin, I.; American Institute of Ultrasound in Medicine Bioeffects Committee. Overview of therapeutic ultrasound applications and safety considerations. *J. Ultrasound Med.* **2012**, *1*, 623–634.
82. Hahm, J. Zinc oxide nanomaterials for biomedical fluorescence detection. *J. Nanosci. Nanotechnol.* **2014**, *14*, 475–486.
83. Ancona, A.; Troia, A.; Garino, N.; Dumontel, B.; Cauda, V.; Canavese, G. Leveraging re-chargeable nanobubbles on amine-functionalized ZnO nanocrystals for sustained ultrasound cavitation towards echographic imaging. *J. Acoust. Soc. Am.* **2011**, *130*, 3184–3208.
84. Byun, K.T.; Seo, K.W.; Shim, I.W.; Kwak, H.Y. Syntheses of ZnO and ZnO-coated TiO₂ nanoparticles in various alcohol solutions at multibubble sonoluminescence (MBSL) condition. *Chem. Eng. J.* **2008**, *135*, 168–173.
85. Goryacheva, I.Y.; Sapelkin, A.V.; Sukhorukov, G.B. Carbon nanodots: Mechanisms of photoluminescence and principles of application. *TrAC-Trends Anal. Chem.* **2017**, *90*, 27–37.
86. Righetto, M.; Carraro, F.; Privitera, A.; Marafon, G.; Moretto, A.; Ferrante, C. The elusive nature of carbon nanodot fluorescence: an unconventional perspective. *J. Phys. Chem. C* **2020**, *124*, 22314–22320.
87. Rivas, D.F.; Ashokkumar, M.; Leong, T.; Yasui, K.; Tuziuti, T.; Kentish, S.; Lohse, D.; Gardeniers, H.J.G.E. Sonoluminescence and sonochemiluminescence from a microreactor. *Ultrason. Sonochem.* **2012**, *19*, 1252–1259.
88. Lu, Y.; Hu, Q.; Lin, Y.; Pacardo, D.B.; Wang, C.; Sun, W.; Ligler, F.S.; Dickey, M.D.; Gu, Z. Transformable liquid-metal nanomedicine. *Nat. Commun.* **2015**, *6*, 10066.
89. Dickey, M.D. Stretchable and soft electronics using liquid metals. *Adv. Mater.* **2017**, *29*, 1606425.
90. Daeneke, T.; Khoshmanesh, K.; Mahmood, N.; Castro, I.A.D.; Esrafilzadeh, D.; Barrow, S.; Dickey, M.; Zadeh, K.K. Liquid metals: fundamentals and applications in chemistry. *Chem. Soc. Rev.* **2018**, *47*, 4073–4111.

91. Reineck, P.; Lin, Y.; Gibson, B.C.; Dickey, M.D.; Greentree, A.D.; Maksymov, I.S. UV plasmonic properties of colloidal liquid-metal eutectic gallium-indium alloy nanoparticles. *Sci. Rep.* **2019**, *9*, 5345.
92. Enoch, S.; Bonod, N. *Plasmonics: From Basic to Advanced Topics*; Springer, Berlin, 2012.
93. Chen, J.; Albella, P.; Pirzadeh, Z.; Alonso-González, P.; Huth, F.; Bonetti, S.; Bonanni, V.; Åkerman, J.; Nogués, J.; Vavassori, P.; Dmitriev, A.; Aizpurua, J.; Hillenbrand, R. Plasmonic nickel nanoantennas. *Small* **2011**, *7*, 2341–2347.
94. Bonanni, V.; Bonetti, S.; Pakizeh, T.; Pirzadeh, Z.; Chen, J.; Nogués, J.; Vavassori, P.; Hillenbrand, R.; Åkerman, J.; Dmitriev, A. Designer magnetoplasmonics with nickel nanoferrromagnets. *Nano Lett.* **2011**, *11*, 5333–5338.
95. Maksymov, I.S.; Greentree, A.D. Dynamically reconfigurable plasmon resonances enabled by capillary oscillations of liquid-metal nanodroplets. *Phys. Rev. A* **2017**, *96*, 043829.
96. Fong, S.W.; Klaseboer, E.; Turangan, C.K.; Khoo, B.C.; Hung, K.C. Numerical analysis of a gas bubble near bio-materials in an ultrasound field. *Ultrasound Med. Biol.* **2006**, *32*, 925–942.
97. Curtiss, G.A.; Leppinen, D.M.; Wang, Q.X.; Blake, J.R. Ultrasonic cavitation near a tissue layer. *J. Fluid Mech.* **2013**, *730*, 245–272.
98. Boyd, B.; Becker, S. Numerical modelling of an acoustically-driven bubble collapse near a solid boundary. *Fluid Dyn. Res.* **2018**, *50*, 065506.
99. Boyd, B.; Becker, S. Numerical modeling of the acoustically driven growth and collapse of a cavitation bubble near a wall. *Phys. Fluids* **2019**, *31*, 032102.
100. Bolton, J.; Colton, C. *The Ultraviolet Disinfection Handbook*; American Water Works Association, 2008.
101. Convery, N.; Gadegaard, N. 30 years of microfluidics. *Micro Nano Eng.* **2019**, *2*, 76–91.
102. Chen, C.; Zhu, Y.; Leech, P.W.; Manasseh, R. Production of monodispersed micron-sized bubbles at high rates in a microfluidic device. *Appl. Phys. Lett.* **2009**, *95*, 144101.
103. Rabaud, D.; Thibault, P.; Mathieu, M.; Marmottant, P. Acoustically bound microfluidic bubble crystals. *Phys. Rev. Lett.* **2011**, *106*, 134501.
104. Zhou, Y.; Seshia, A.A.; Hall, E.A.H. Microfluidics-based acoustic microbubble biosensor. SENSORS, IEEE, USA, 2013, pp. 1–4. doi:10.1109/ICSENS.2013.6688408.
105. Maksymov, I.S.; Greentree, A.D. Synthesis of discrete phase-coherent optical spectra from nonlinear ultrasound. *Opt. Express* **2017**, *25*, 7496–7506.
106. Toegel, R.; Luther, S.; Lohse, D. Viscosity destabilizes sonoluminescing bubbles. *Phys. Rev. Lett.* **2006**, *96*, 114301.
107. Lu, X.; Prosperetti, A.; Toegel, R.; Lohse, D. Harmonic enhancement of single-bubble sonoluminescence. *Phys. Rev. E* **2003**, *67*, 056310.
108. Nguyen, B.Q.H.; Maksymov, I.S.; Suslov, S.A. Acoustic frequency combs using gas bubble cluster oscillations in liquids: a proof of concept. *Sci. Reps.* **2021**, *11*, 38.
109. Maksymov, I.S.; Besbes, M.; Hugonin, J.P.; Yang, J.; Beveratos, A.; Sagnes, I.; Robert-Philip, I.; Lalanne, P. Metal-coated nanocylinder cavity for broadband nonclassical light emission. *Phys. Rev. Lett.* **2010**, *105*, 180502.
110. Sauvan, C.; Hugonin, J.P.; Maksymov, I.S.; Lalanne, P. Theory of the spontaneous optical emission of nanosize photonic and plasmon resonators. *Phys. Rev. Lett.* **2013**, *110*, 237401.
111. Akselrod, G.M.; Argyropoulos, C.; Hoang, T.B.; Ciraci, C.; Fang, C.; Huang, J.; Smith, D.R.; Mikkelsen, M.H. Probing the mechanisms of large Purcell enhancement in plasmonic nanoantenna. *Nat. Photon.* **2014**, *8*, 835–840.
112. Krasnok, A.E.; Slobozhanyuk, A.P.; Simovski, C.R.; Tretyakov, S.A.; Poddubny, A.N.; Miroshnichenko, A.E.; Kivshar, Y.S.; Belov, P.A. An antenna model for the Purcell effect. *Sci. Reps.* **2015**, *5*, 12956.
113. Eberlein, C. Theory of quantum radiation observed as sonoluminescence. *Phys. Rev. A* **1996**, *53*, 2772–2787.
114. Eberlein, C. Sonoluminescence as quantum vacuum radiation. *Phys. Rev. Lett* **1996**, *76*, 3842–3845.
115. Maksymov, I.S.; Greentree, A.D. Acoustically tunable optical transmission through a subwavelength hole with a bubble. *Phys. Rev. A* **2017**, *95*, 033811.
116. Landi, M.; Zhao, J.; Prather, W.E.; Wu, Y.; Zhang, L. Acoustic Purcell effect for enhanced emission. *Phys. Rev. Lett.* **2018**, *120*, 114301.
117. Schmidt, M.K.; Helt, L.G.; Poulton, C.G.; Steel, M.J. Elastic Purcell effect. *Phys. Rev. Lett.* **2018**, *121*, 064301.
118. Schmidt, M.K.; Helt, L.G.; Poulton, C.G.; Steel, M.J. Harnessing simultaneous optical and acoustic Purcell effects. 3rd International Workshop on Optomechanics and Brillouin Scattering (WOMBAT 3), Tel-Aviv, Israel, March 26–28, 2019.
119. Zheludev, N.I.; Kivshar, Y.S. From metamaterials to metadevices. *Nat. Mater.* **2012**, *11*, 917–924.
120. Poddubny, A.; Iorsh, I.; Belov, P.; Kivshar, Y. Hyperbolic metamaterials. *Nat. Photon.* **2013**, *7*, 948–957.
121. Trigo, M.; Bruchhausen, A.; Fainstein, A.; Jusserand, B.; Thierry-Mieg, V. Confinement of acoustical vibrations in a semiconductor planar phonon cavity. *Phys. Rev. Lett.* **2002**, *89*, 227402.
122. Smolyaninov, I.I.; Smolyaninova, V.N. Analogue quantum gravity in hyperbolic metamaterials. *Universe* **2022**, *8*, 242.
123. Smolyaninov, I.I.; Smolyaninova, V.N. Fine tuning and MOND in a metamaterial “multiverse”. *Sci. Reps.* **2017**, *7*, 8023.